Properties of the nitrogen acceptor in ZnO

Martin Straßburg[1], U. Haboeck[1], A. Kaschner[1], Matthias Straßburg[1], A. Rodina[1], A. Hoffmann[1], C. Thomsen[1], A. Zeuner[2], H.R. Alves[2], D.M. Hofmann[2], and B.K. Meyer[2]

[1] Institut für Festkörperphysik, Technische Universität Berlin, Hardenbergstr.36, 10623 Berlin, Germany

[2] I. Physikalisches Institut, Justus-Liebig-Universität Gießen, Heinrich-Buff-Ring 16, 35392 Gießen, Germany

Abstract. We study the incorporation of nitrogen into ZnO. A series of samples grown by chemical vapour deposition (CVD) containing different nitrogen concentrations, as determined by secondary ion mass spectroscopy (SIMS), was investigated. Nitrogen forms a shallow acceptor in ZnO and leads to typical excitonic emission and donor-acceptor pair band recombination. Binding energies of ~16 meV for the exciton and ~165 meV for the nitrogen acceptor are obtained. The Raman spectra revealed local vibrational modes at 275, 510, 582, 643 and 856 cm^{-1} in addition to the host phonons of ZnO. The intensity of these additional modes correlates linearly with the nitrogen concentration and can be used as a quantitative measure of nitrogen in ZnO. Furthermore, SIMS showed a correlation between the concentration of incorporated nitrogen and unintentional hydrogen. This hints to the origin of compensated acceptor states detected in PL measurements. The compensation mechanisms may be similar to those reported for GaN:Mg.

1. Introduction

There is rising interest in investigating the properties of ZnO epitaxial films due to its superior properties such as high exciton binding energy combined with low lasing threshold density [1] and good resistance to bombardment with high-energy particles [2,3]. The material is a potential competitor for GaN-based light-emitting devices in the ultraviolet and blue spectral range. Like for other wide-band gap semiconductors as GaN [4] and ZnSe [5] controlled p-type doping is difficult. However, there have been reports on the synthesis of p-conducting ZnO doped with As [6] and a Ga/N co-doping [7] as well as the fabrication of a p-n-junction by excimer-laser doping [8].

We report on doping experiments with nitrogen as a potential acceptor and its influence on the photoluminescence (PL) properties and lattice dynamics of ZnO. A series of samples grown by chemical vapour deposition. The nitrogen concentrations in these samples were varied by the growth conditions and obtained by secondary ion mass spectroscopy (SIMS). Exciton binding energy as well as the energy position of the nitrogen acceptor above the valence band were determined.

2. Experimental Details

The ZnO samples were grown by chemical vapour deposition (CVD) using a home built epitaxy system which consists of a horizontal quartz reactor and a resistance heating with different temperature zones. Metallic zinc was kept in one zone at a temperature of 470°C. The growth temperature was 650°C. We used NO_2 as oxygen precursor and NH_3 as nitrogen source for the doping experiments. The epitaxial films were deposited on GaN/Sapphire templates which offers the advantage of a lattice parameter similar to ZnO. The thickness of deposited ZnO was determined to ~10µm.

Photoluminescence (PL) was excited by the 325 nm line of a HeCd-laser. The samples were mounted in a cryostat allowing the variation of temperatures between 2 K and 300 K. The spectral resolution of the detection system was better than 0.2 meV. The Raman-scattering experiments were carried out in backscattering geometry with a triple-grating spectrometer equipped with a cooled charge-coupled device detector. The lines at 488 nm and 514.5 nm of an Ar^+/Kr^+ mixed-gas laser were used for excitation. The line positions were determined with an accuracy better than 1 cm^{-1}. Secondary ion mass spectroscopy (SIMS) was applied to determine the concentration of nitrogen and unintentional dopants such as hydrogen. The primary ion species was caesium. Nitrogen was detected as $^{14}N^{16}O^-$ and hydrogen as $^{64}Zn^1H^-$ clusters. The given absolute concentrations are accurate to within half an order of magnitude. Despite this accuracy the relative error is less than 10%.

3. Results and Discussion

In total we investigated five samples with different nitrogen concentration as estimated from the growth parameters. SIMS investigations were performed to achieve the nitrogen concentration (see figure 1). The nitrogen concentration was deduced from the signal intensity of the NO^- cluster consisting of ^{14}N and ^{16}O isotopes. The detection limit of this method is around 10^{17} cm^{-3}. The nitrogen concentration increases from sample B to E with a maximum concentration of about 10^{19} cm^{-3}. Sample A is undoped.

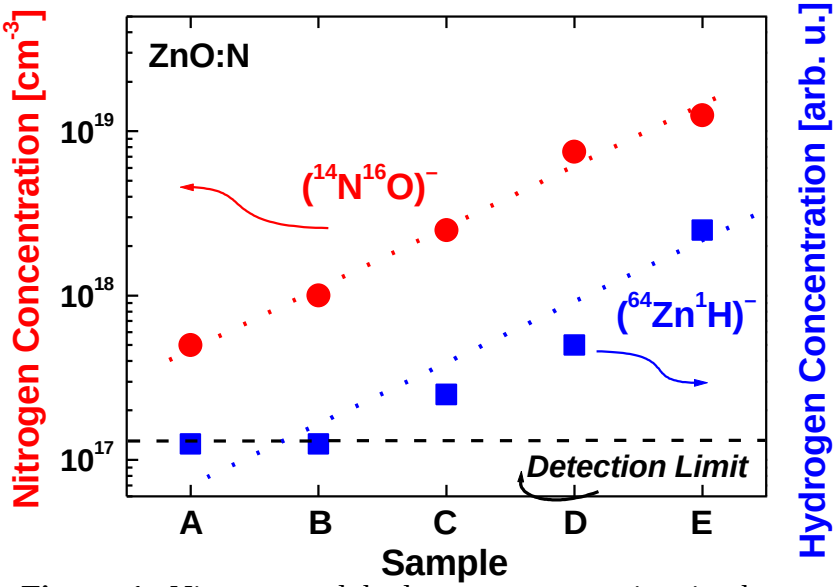

Figure 1. Nitrogen and hydrogen concentration in the samples under investigation as determined from SIMS. The nitrogen concentration increases from sample A to E. The hydrogen concentration linearly correlates with the nitrogen concentration. The dotted lines are drawn as a guide to the eye.

Simultaneously, the hydrogen concentration as detected by the $^{64}Zn^{1}H^{-}$ cluster linearly increases with the nitrogen content. Since we do not have a calibration standard for hydrogen, a quantitative scaling of the hydrogen concentration is unfortunately not possible. Nevertheless, a qualitative comparison of the samples can be given. A higher nitrogen concentration seems to drive the material to build in a higher concentration of compensating hydrogen. A similar mechanism as for GaN, where the concentration of magnesium acting as an acceptor and compensating hydrogen are linearly correlated [9], may be the reason for this behaviour. This fact may have a strong impact on the compensation mechanism in ZnO. To study the properties of the incorporated nitrogen in detail, Raman and PL spectroscopy investigations were performed.

3.1. Local vibrational modes of nitrogen in ZnO

Figure 2 exhibits Raman spectra of samples A to E. Sample A is undoped ZnO, and the estimated nitrogen concentration increases from sample B to sample E. Beside the expected E_2(low) and E_2(high) mode of ZnO we find a variety of other modes, which need to be explained. At 569 cm^{-1} we find the E_2(high) mode of the GaN template. The feature at 332 cm^{-1} is a second-order structure of ZnO, which was interpreted as $2E_2$(M) [10]. There are five more modes with frequencies of 275, 510, 582, 643 and 856 cm^{-1} which do not belong to first- or second-order structures of ZnO or the GaN template material. The mode at 582 cm^{-1} was already found in ZnO:N by X. Wang *et al.* and interpreted as A_1(LO) mode [11]. Whereas they gave no explanation for the four remaining Raman modes, but suggested that these modes may be related to nitrogen doping. We also find a well-resolved 582 cm^{-1} mode having a high intensity. Because the A_1(LO) mode is not allowed in backscattering configuration with crossed polarization we conclude that it is not the A_1(LO) mode of ZnO. However, we agree that all of the additional modes are nitrogen-related. Neither of the additional modes are found in undoped material. Also in ZnO:Ga (not shown) none of these Raman modes was

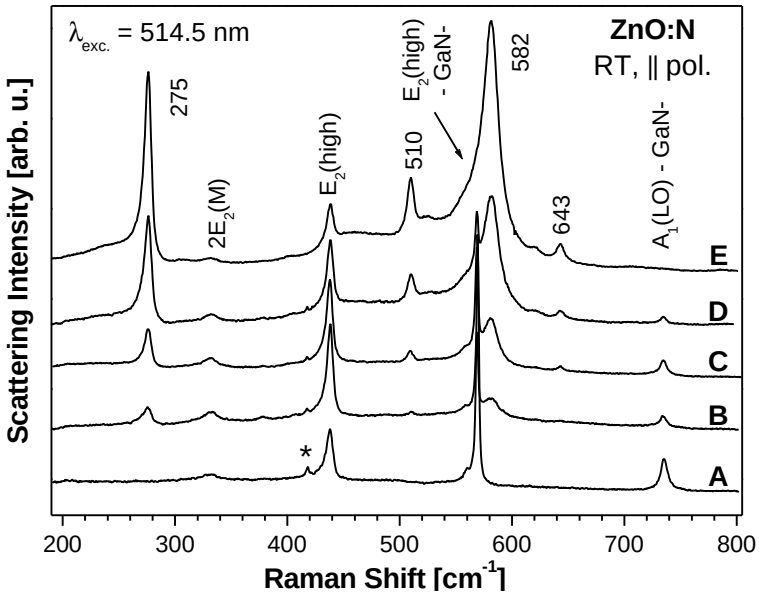

Figure 2. Room temperature Raman spectra of five ZnO samples. Sample A is undoped, whereas the nitrogen concentration increases from sample B to E. Raman modes marked by their wavenumber are interpreted as local vibrational modes. The peak marked by an asterisk originates from the sapphire substrate.

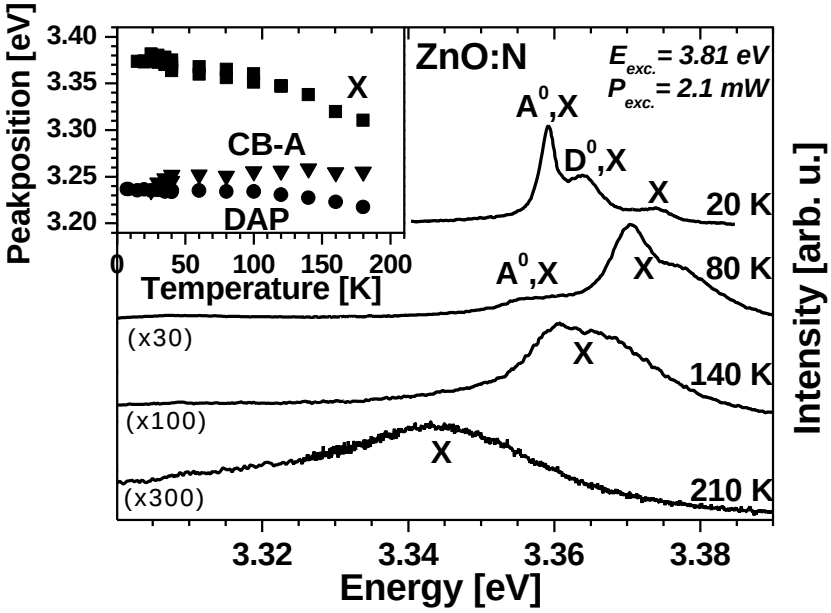

Figure 3. Near bandedge photoluminescence spectra recorded at various temperatures. Acceptor- (A^0,X) and donor-bound (D^0,X) excitons are marked at the respective peaks. Due to its larger binding energy the free exciton (X) remains observable up to elevated temperatures. The inset shows the temperature dependence of the free exciton and the donor-acceptor-pair band (DAP) and the band-acceptor (CB-A) recombination.

observed.

The intensity of the five modes increases with nitrogen concentration (from sample B to E). Furthermore, the intensity of the A_1(LO) mode from the GaN template subsequently decreases from A to E. This results from the higher absorption in the visible spectral range with increasing nitrogen concentration [11]. The correlation of the mode intensities and the nitrogen concentration leads to the conclusion that all the additional modes are LVMs of nitrogen in ZnO. Another possible explanation could be that these modes originate from regions with a high density of states which can be observed in first-order Raman spectra of highly defective material [12]. There are a few arguments against this assignment. First, is the comparison with the calculated PDOS [13]. Second, there are no signs of an inferior material quality of the doped ZnO. For instance the full width at half maximum of the E_2(high) mode in ZnO is 6 - 7 cm^{-1}. This value is independent from the doping level.

3.2. Photoluminescence properties and binding energy of nitrogen

The optical properties are investigated by temperature dependent PL. Figure 3 shows the near bandedge emission and its temperature dependence. Near the bandedge two prominent bound excitons can be resolved, at 3.363 eV the I_4 neutral donor bound exciton line and at 3.36 eV the neutral acceptor bound exciton line of $I_{7/8}$ [14]. A third weak transition at 3.33 eV is tentatively assigned to deeply bound excitons at structural defects. In addition, with a factor of 30 less intense a well structured donor-acceptor-pair (DAP) transitions is observed with a zero phonon line (ZPL) at 3.235 eV. The ZPL is followed by four LO phonon replicas (not shown here). The weak DAP emission

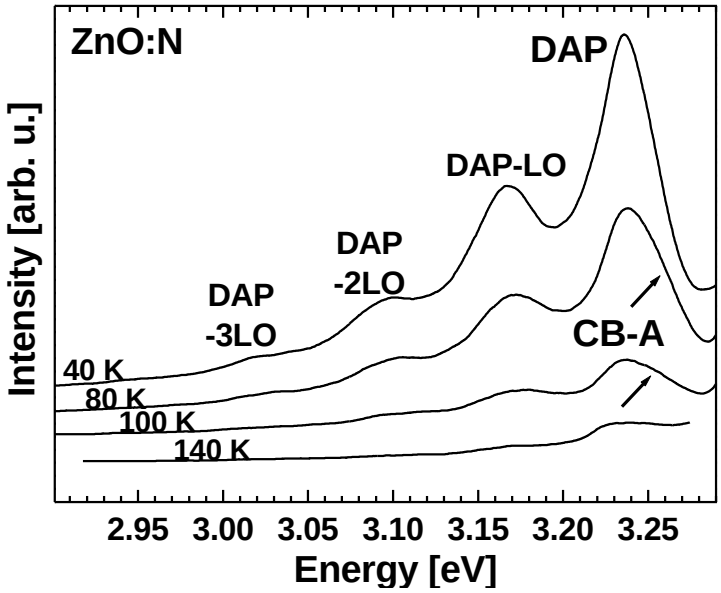

Figure 4. Photoluminescence spectra in the DAP range taken at four different temperatures. The pronounced LO-phonon replica of the DAP bands indicating a high Huang-Rhys factor.

intensity points to compensation of acceptor states, as confirmed by hydrogen incorporation detected in SIMS investigations mentioned above.

In the inset of figure 3 the temperature dependence of the emission energy of various emission bands is depicted.

With a factor 30 less in intensity a DAP recombination followed by several LO phonon replica is observed (figure 4). Its zero phonon line (ZPL) peaks at 3.235 eV and it is repeated by longitudinal optical phonon replicas with an energy of 73 meV. Note that in undoped ZnO (not shown here) the ZPL is at 3.22 eV. The recombination of an electron with a hole leads to the emission of phonons caused by the electron (hole) - phonon interaction. In case of strong phonon-coupling, i.e. strong interaction with the lattice, several replicas can be observed. Their intensities can be described by a simple Poisson distribution

$$I_n = I_{ZPL} \frac{N^n}{n!}, \tag{1}$$

with I_n is the intensity of the n^{th} phonon replica, and N is the mean number of created phonons (or Huang Rhys factor). The mean number of created phonons is proportional to the binding energy of the acceptor E_A according to model of Hopfield

$$N = E_A \frac{2e_S}{hw_{LO}\,2p \cdot 1/2\left(\frac{1}{e_S} - \frac{1}{e_0}\right)}, \tag{2}$$

with e_s and e_0 the static and high frequency dielectric constants 3.75 and 8.75 respectively, and $h\omega_{LO}$ being the phonon energy of 73 meV in ZnO. Hence, with a Huang-Rhys factor of 0.85 determined from PL measurements a binding energy of 136 meV for the nitrogen acceptor is obtained.

To improve the above introduced calculation temperature-dependent investigations (see inset of figure 3 and figure 4) of the DAP-photoluminescence compared to the free

exciton line were performed. Above 30 K the contribution of the band-acceptor (CB-A) recombination rises benefiting from the small binding energy of the donor-bound exciton complex. From the energetic distance between the DAP ZPL and the CB-A-transition at 50 K we can estimate the residual donor concentration to be N_D=10^{17} cm^{-3}. Using a donor binding energy of 54 meV and

$$E_A = \left(E_{gap} - E_D\right) - \left(E\left(D^0, A^0\right) - aN_D^{1/3}\right), \tag{3}$$

we determine the acceptor binding energy E_A to be 163 ± 5 meV, where with E_D is the shallow donor binding energy and N_D is its concentration. For α= 3x10^{-5} meVcm was used. Note that for the residual acceptor in ZnO the ionisation energy is approx. 30 meV larger [15].

Furthermore, the binding energy of the nitrogen acceptor can be also derived from the binding energy of the bound exciton by using Hayne's rule [16]. Exciton binding energy could be obtained by either the spectral position of free and bound exciton or the temperature dependence of the PL intensity. The luminescence of excitons bound to neutral nitrogen acceptor was observed at 3.3598 eV (see figure 3). Its localisation energy of 15.9 meV was derived from the PL maximum of the free exciton. The value is in very good agreement with the activation energy of 16 meV determined from temperature dependence of the PL intensity, which is shown in figure 5. In the latter case the activation energy E_{act} of the nitrogen bound exciton is obtained by

$$I(T) = const. \cdot \frac{1}{\exp\left(\frac{-E_{act}}{kT}\right)}, \tag{4}$$

where I is the PL intensity, k the Bolzmann factor and T the temperature.

The nitrogen acceptor bound exciton in ZnSe has a localization energy of 10 meV. The ratio of localization energy to the acceptor binding energy of 110 meV is hence

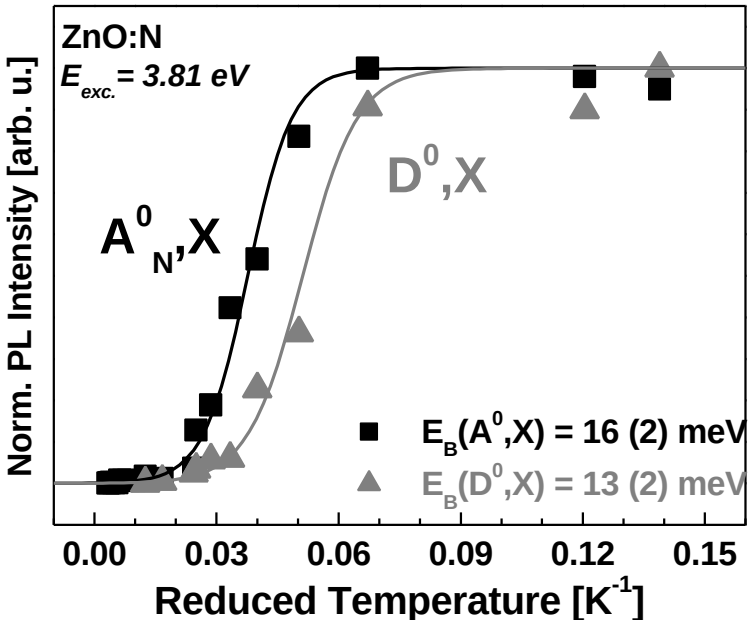

Figure 5. Normalized photoluminescence intensity of the donor- and acceptor-bound exciton lines as function of temperature in ZnO: N. The straight lines represent fits to obtain the activation energy using equation (4).

0.091. In ZnO we find (figure 3 and 5) the nitrogen acceptor bound exciton to have a localization energy of 16 meV. This value leads to the shallow nitrogen acceptor binding energy of 165 meV using a factor of 0.097 which is derived from an other acceptor-bound exciton in ZnO. The bound exciton line I_9 [15] often correlated with Na has a binding energy of 19 meV. Whereas the corresponding acceptor state has a binding energy of 195 meV.
To our knowledge, this is the first report on the optical signature of the shallow nitrogen acceptor in ZnO. The estimated binding energy for the nitrogen acceptor is somewhat lower than Mg in GaN.

4. Conclusion

In summary, nitrogen-doped ZnO samples grown by CVD with different concentrations of nitrogen were investigated. The nitrogen and hydrogen concentrations were determined by secondary ion mass spectroscopy. In addition to the host phonons of ZnO we found modes at 275, 510, 582, 643 and 856 cm^{-1} in the Raman spectra of these samples. All five modes scale in intensity with nitrogen content and are interpreted in terms of nitrogen-related local vibrational modes. Furthermore, a linear correlation between the nitrogen and hydrogen concentration in the samples was found. This could have strong influence on the compensation mechanism in CVD-grown ZnO. Compensation of acceptor states are confirmed by photoluminescence (PL) investigations, where the intensity of the donor-acceptor pair band was 30 times less than the intensity of the exciton emission lines. Additionally, temperature-dependent PL investigations enabled the determination of the binding energy of nitrogen-bound exciton (16 meV). The binding energy of the nitrogen acceptor was determined to ~165 meV. This is considerably lower than Mg in GaN, and once overcoming compensation mechanisms nitrogen is a promising candidate to reach higher hole densities at lower doping levels in ZnO.

References

1 D. M. Bagnall, Y. F. Chen, Z. Zhu, T. Yao, S. Koyama, M. Y. Shen, and T. Goto, Appl. Phys. Lett. **70**, 2230 (1997)
2 D. C. Look, D. C. Reynolds, J. W. Hemsky, R. L. Jones, and J. R. Sizelove, Appl. Phys. Lett. **75**, 811 (1999)
3 F. D. Auret, S. A. Goodman, M. Hayes, M. J. Legodi, H.A. van Laarhoven, and D. C. Look, Appl. Phys. Lett. **79**, 3074 (2001)
4 H. Amano, M. Kito, K. Hiramatsu, and I. Akasaki, Jpn. J. Appl. Phys., Part 2 **28**, L2112 (1989)
5 R. Heitz, E. Moll, V. Kutzer, D. Wiesmann, B. Lummer, A. Hoffmann, I. Broser, P. Bäume, W. Taudt, J. Söllner, and M. Heuken, J. Cryst. Growth **159**, 307 (1996)
6 Y. R. Ryu, S. Zhu, D. C. Look, J. M. Wrobel, H. M. Jeong, and H. W. White, J. Cryst. Growth **216**, 330 (2000)
7 M. Joseph, H. Tabata, and T. Kawai, Jpn. J. Appl. Phys., Part 2 **38**, L1205 (1999)
8 T. Aoki, Y. Hatanka, and D. C. Look, Appl. Phys. Lett. **76**, 3257 (2000)
9 L. Sugiura, M. Suzuki, and J. Nishio, Appl. Phys. Lett. **72**, 1748 (1998)
10 J. M. Calleja and M. Cardona, Phys. Rev. B **16**, 3753 (1977)
11 X. Wang, S. Yang, J. Wang, M. Li, X. Jiang, G. Du, X. Liu, and R. P. H. Chang, J. Cryst. Growth **226**, 123 (2001)
12 V. Yu. Davydov, Yu. E. Kitaev, I. N. Goncharuk, A. N. Smirnov, J. Graul, O. Semchinova, D. Uffmann, M. B. Smirnov, A. P. Mirgorodsky, and R. A. Evarestov, Phys. Rev. B **58**, 12899 (1998)

13 A. Kaschner, U. Haboeck, Martin Strassburg, Matthias Strassburg, G. Kaczmarczyk, A. Hoffmann, C. Thomsen, A. Zeuner, H.R. Alves, D.M. Hofmann, B.K. Meyer, Appl. Phys. Lett. **80**, 1909 (2002)
14 This assignment is given in: C. Klingshirn, phys. stat. sol. (b) **71**, 547 (1975) and J. Gutowski, N. Presser, and I. Broser, Phys. Rev. B **38**, 9746 (1988)
15 E. Tomzig and R. Helbig, J. Lumin. **14**, 403 (1976)
16 J.R. Haynes, Phys. Rev. Lett. **4**, 361 (1960)